

2011

Magnetoresistance, critical current density, and magnetic flux pinning mechanism in nickel doped BaFe₂As₂ single crystals

Mahboobeh Shahbazi
University of Wollongong, msm979@uow.edu.au

Xiaolin Wang
University of Wollongong, xiaolin@uow.edu.au

Z W. Lin
Univ Technol Sydney

J G. Zhu
Univ Technol Sydney

S. X. Dou
University of Wollongong, shi@uow.edu.au

See next page for additional authors

Follow this and additional works at: <https://ro.uow.edu.au/engpapers>

 Part of the [Engineering Commons](#)

<https://ro.uow.edu.au/engpapers/1373>

Recommended Citation

Shahbazi, Mahboobeh; Wang, Xiaolin; Lin, Z W.; Zhu, J G.; Dou, S. X.; and Choi, K Y.: Magnetoresistance, critical current density, and magnetic flux pinning mechanism in nickel doped BaFe₂As₂ single crystals 2011.
<https://ro.uow.edu.au/engpapers/1373>

Authors

Mahboobeh Shahbazi, Xiaolin Wang, Z W. Lin, J G. Zhu, S. X. Dou, and K Y. Choi

Magnetoresistance, critical current density, and magnetic flux pinning mechanism in nickel doped BaFe₂As₂ single crystals

M. Shahbazi, X. L. Wang, Z. W. Lin, J. G. Zhu, S. X. Dou et al.

Citation: *J. Appl. Phys.* **109**, 07E151 (2011); doi: 10.1063/1.3563057

View online: <http://dx.doi.org/10.1063/1.3563057>

View Table of Contents: <http://jap.aip.org/resource/1/JAPIAU/v109/i7>

Published by the [American Institute of Physics](#).

Related Articles

Magnetic and superconducting properties of spin-fluctuation-limited superconducting nanoscale VN_x
J. Appl. Phys. **111**, 07E142 (2012)

Annealing effect on the excess conductivity of Cu_{0.5}Ti_{0.25}M_{0.25}Ba₂Ca₂Cu₃O_{10-δ} (M=K, Na, Li, Ti) superconductors
J. Appl. Phys. **111**, 053914 (2012)

Effect of columnar grain boundaries on flux pinning in MgB₂ films
J. Appl. Phys. **111**, 053906 (2012)

The scaling analysis on effective activation energy in HgBa₂Ca₂Cu₃O_{8+δ}
J. Appl. Phys. **111**, 07D709 (2012)

Magnetism and superconductivity in the Heusler alloy Pd₂YbPb
J. Appl. Phys. **111**, 07E111 (2012)

Additional information on J. Appl. Phys.

Journal Homepage: <http://jap.aip.org/>

Journal Information: http://jap.aip.org/about/about_the_journal

Top downloads: http://jap.aip.org/features/most_downloaded

Information for Authors: <http://jap.aip.org/authors>

ADVERTISEMENT



**FIND THE NEEDLE IN THE
HIRING HAYSTACK**

Post jobs and reach
thousands of hard-to-find
scientists with specific skills



<http://careers.physicstoday.org/post.cfm> **physicstoday JOBS**

Magnetoresistance, critical current density, and magnetic flux pinning mechanism in nickel doped BaFe₂As₂ single crystals

M. Shahbazi,¹ X. L. Wang,^{1,a)} Z. W. Lin,² J. G. Zhu,² S. X. Dou,¹ and K. Y. Choi³

¹*Institute for Superconducting and Electronic Materials, University of Wollongong, Innovation Campus, Australian Institute for Innovative Materials, Squires Way, Fairy Meadow, NSW 2519, Australia*

²*Department of Engineering and Information Technology, University of Technology, Sydney, City Campus, P. O. Box 123, Broadway, NSW 2007, Australia*

³*Department of Physics, Sogang University, Seoul 121-742, Republic of Korea*

(Presented 16 November 2010; received 24 September 2010; accepted 15 December 2010; published online 8 April 2011)

The critical current density, J_c , flux pinning behavior and magnetoresistance results of BaFe_{2-x}Ni_xAs₂ single crystal have been investigated in fields up to 13 T over a temperature range of 2 to 20 K. The magnetoresistance below the superconducting transition temperature (T_c) shows Arrhenius thermally activated behavior: $\rho = \rho_o \exp(-U_o(T,H)/k_B T)$, where U_o is the thermally activated energy. BaFe_{2-x}Ni_xAs₂ exhibits high thermally activated flux flow energy with a very weak field dependence. J_c is as high as 2×10^5 A/cm² for zero magnetic field at 2 K. J_c was found to decrease for $B < 1$ T, but showed a very weak field dependence and remained nearly constant with increasing magnetic field for $B > 1$ T at $T = 2, 5$, and 10 K. Flux jumping was also observed in magnetization loops at very low temperature for large sample, which is related to the high J_c in the single crystal. A peak effect was observed at 10 K. © 2011 American Institute of Physics. [doi:10.1063/1.3563057]

The discovery of the first iron based superconductor, fluorine doped LaFeAsO,¹ aroused great interest due to the high upper critical field H_{c2} , high J_c , and very high intrinsic pinning potential compared with MgB₂ and other conventional superconductors and even cuprate superconductors. Doped BaFe₂As₂ has a maximum T_c of 38 K. The parent compound shows an anomalous decrease in the resistivity at $T = 140$ K, which is related to structural change combined with spin density wave transition,²⁻⁴ and superconductivity occurs by hole doping with alkali metals such as Na,⁵ K,⁶ or Cs,⁷ or by electron doping achieved by replacing a small fraction of Fe with a large transition metal ion.⁸⁻¹²

A second peak effect has been observed in BaFe_{2-x}Co_xAs₂,¹³⁻¹⁶ BaFe_{2-x}Ni_xAs₂¹³ and Ba_{1-x}K_xFe₂As₂ single crystal.^{13,17} The second peak effect can be resulted by a crossover from the elastic collective creep to the plastic vortex creep¹³ or it is associated with the structural phase transition from a rhomb lattice at low field to a square lattice above a transition field.¹⁵ The absence of the second magnetization peak effect in CaFe_{2-x}Co_xAs₂ indicated that the vortex dynamics in this compound is consistent with plastic creeping rather than the collective creep model.¹⁸

(Ba,K)Fe₂As₂ superconductor with nearly isotropic superconductivity,¹⁹ very high intrinsic pinning,²⁰ H_{c2} as high as 200 T, and high pinning potential, as high as 10^4 K²⁰ is a promising candidate for high magnetic field application. Flux jumping has been also observed in the Ba_{1-x}K_xFe₂As₂ single crystal.²⁰ However, flux jumping and pinning potential behavior have not been reported in the electron doped BaFe_{2-x}Ni_xAs₂ so far. In this paper we present the pinning potential behavior in optimal electron doped BaFe_{1.9}Ni_{0.1}As₂

single crystal. The pinning potential is as high as 5300 K at low magnetic field for both ab plane and c direction. Estimated H_{c2} from the slope of dH_{c2}/dT is $H_{c2}^{ab} = 81.5$ T, which higher than the Bardeen–Cooper–Schrieffer (BCS) paramagnetic limit. Flux jumping is observed at low temperature and low magnetic field.

Single crystal with the nominal composition BaFe_{1.9}Ni_{0.1}As₂ was prepared by a self-flux method. Details of the single crystal growth will be reported elsewhere. The as-grown single crystal was cleaved and cut into a rectangular shape for measurement. The transport properties were measured over a wide range of temperature and magnetic fields up to 13 T with applied current of 5 mA using a physical properties measurement system (PPMS, Quantum Design). The temperature dependence of the magnetization and the M - H loops were measured using magnetic properties measurement system (MPMS, Quantum Design). The critical current density was calculated using the Bean model.

The temperature dependence of the resistivity of BaFe_{1.9}Ni_{0.1}As₂ for applied field parallel to the ab plane and c direction is shown in Fig. 1. The resistivity decreases with decreasing temperature from 300 to 19.4 K, supporting metallic behavior of this compound for $H//c$. The resistance drops to zero at $T_c^{\text{on}} = 17.6$ K for $H//c$ in zero magnetic field. The T_c value is lower than that reported in Ref. 21. The onset of superconductivity slowly shifts to lower temperature with increasing magnetic field, which is related to the nearly isotropic superconductivity in the 122 family.²² The superconducting transition width, $\Delta T_c = 0.8$ K, was calculated using the temperature difference between the 90% and 10% values in the drop-off of the resistivity at zero magnetic field, which indicates a sharp superconducting transition temperature and high quality single crystal.

^{a)}Electronic mail: xiaolin@uow.edu.au.

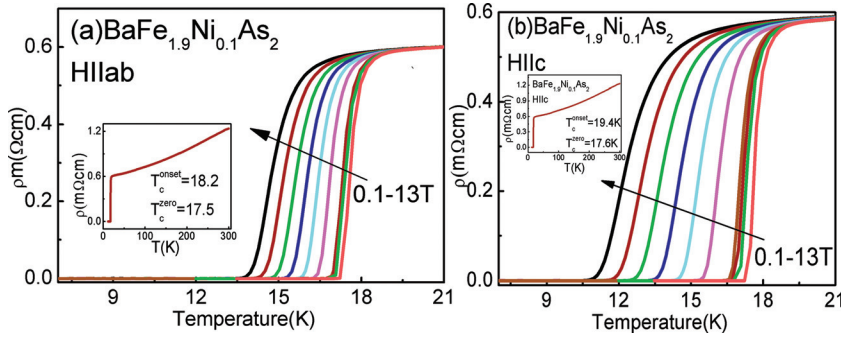


FIG. 1. (Color online) Temperature dependence of resistivity of a $\text{BaFe}_{1.9}\text{Ni}_{0.1}\text{As}_2$ single crystal in different magnetic field up to 13 T.

H_{c2} is characterized as the field at which the resistance becomes 90% of the normal state resistivity; while the irreversibility field, H_{irr} , is defined by 10% of the normal state resistivity. Figure 2 shows the temperature dependence of H_{c2} and H_{irr} as a function of temperature, based on the magnetoresistance measurement. The estimated slopes for H_{c2} and H_{irr} are -6.09 and -4.22 for $H//c$. Different slopes, dH_{c2}/dT , have been estimated for $\text{BaFe}_{2-x}\text{Ni}_x\text{As}_2$ iron based superconductor ranging from 5.42 TK^{-1} for $x=0.09$ (Ref. 13) to the high value of 9.9 TK^{-1} for $x=0.1$ (Ref. 23) single crystal. H_{c2} was estimated by using the conventional one-band Werthamer–Helfand–Hohenberg (WHH) theory: $H_{c2}(0) = -0.69T_c (dH_{c2}/dT)$, assuming that H_{c2} is limited by the orbital pair breaking effect. The H_{c2} values estimated to be 46.6 and 81.5 T along the ab plane and c direction, respectively. The estimated H_{irr} values are 29.3 and 56.5 T along ab plane and c direction at zero temperature, respectively. The estimated H_{irr} is close to the estimated H_{c2} , which is related to strong vortex pinning or weak thermal fluctuation in this compound.

There are two mechanisms for destroying superconductivity with applying magnetic field. The first one is the orbital effect which is related to the pair breaking of Cooper pairs by the Lorentz force via the charge and the opposite momenta on the Cooper pairs. The other one is the paramagnetic effect where a singlet pair is broken by the Zeeman effect. The estimated upper critical field calculated from the WHH theory is higher than the BCS paramagnetic limit, H_p^{BCS} , in the weak coupling area. By using the weak coupling BCS formula, $H_p^{\text{BCS}} = 1.84 T_c$, we obtain $H_p^{\text{BCS}} = 35.7 \text{ T}$. The estimated H_{c2}^c from the WHH formula is 2.3 times of this limit along c direction showing that the Zeeman paramagnetic pair break-

ing possibly is essential for H_{c2}^{ab} . Also, it reveals the unconventional superconducting mechanism in this family. A similar result was reported for the Co doped 122 family.²⁴ Using the value of H_{c2}^{ab} , we calculated the Ginzburg–Landau coherence length, $\xi_{GL} = (\phi_0/2\pi H_{c2}^c)^{1/2}$ where $\phi_0 = 2.07 \times 10^{-7} \text{ Oe cm}^2$. The obtained coherence length 2.7 and 2.01 nm along ab plane and c direction at $T=0 \text{ K}$, respectively. According to our data, the estimated anisotropy for $\text{BaFe}_{1.9}\text{Ni}_{0.1}\text{As}_2$ is $\gamma = H_{c2}^{ab}/H_{c2}^c = 1.7$, for the temperature range of $12 < T < 18 \text{ K}$ which indicates nearly isotropic superconductivity in this compound.

Thermally activated flux flow is responsible for the broadening of the resistivity transition and can be described by the following equation: $\rho(T, H) = \rho_n \exp(-U_o(T, H)/k_B T)$, where ρ_n is the normal state resistivity, U_o is the pinning potential and k_B is the Boltzmann constant. In Fig. 3, we plot $\log \rho$ vs T^{-1} at different magnetic fields. The linearity of $\log \rho$ vs $1/T$ indicates the thermally activated energy behavior of the resistivity. The slope of the curves is the pinning potential, U_o .

The best fit to the experimental data yields a value of the pinning potential of 5300 K for $H//c$ and $H//ab$ at the low magnetic field of 0.1 T. The pinning potential value for $\text{BaFe}_{1.9}\text{Ni}_{0.1}\text{As}_2$ single crystal is 5 times greater than that of Bi-2212 crystal.²⁵ This value is lower than the reported value of 9100 K for $\text{Ba}_{0.55}\text{K}_{0.45}\text{Fe}_2\text{As}_2$ single crystal for $H//ab$,²⁰ probably due to the different dopants. The magnetic field dependence of the pinning potential is shown in Fig. 4. The activation energy drops very slowly with increasing applied magnetic field for $B < 1 \text{ T}$, scaled as $B^{-0.11}$, and then decreases slowly as $B^{-0.56}$ for $B > 1 \text{ T}$ for $H//c$. This means that the pinning potential is almost field independent for $B < 1 \text{ T}$.

Figure 5 shows the M – H loops measured at 2, 5, 10, and 15 K in the field range of $-5 \text{ T} \leq H \leq 5 \text{ T}$ for

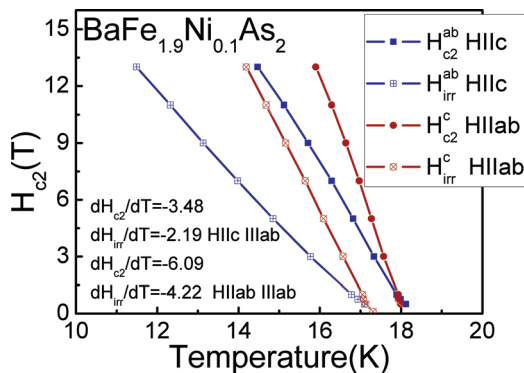


FIG. 2. (Color online) Temperature dependence of the upper critical field and irreversibility field.

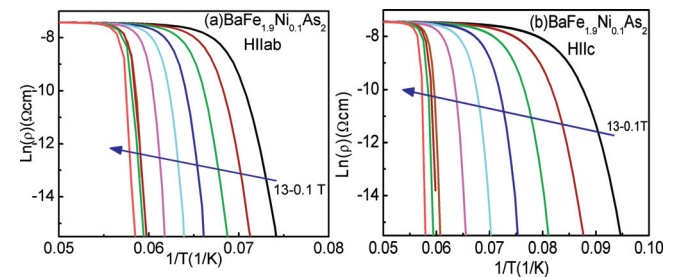


FIG. 3. (Color online) Arrhenius plot of the electrical resistivity at different magnetic fields parallel to the ab plane and c direction.

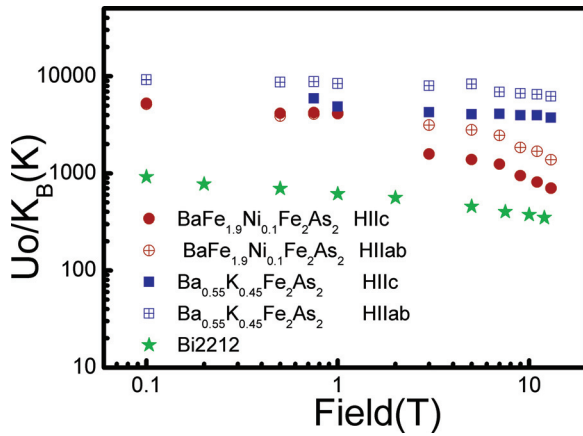


FIG. 4. (Color online) Magnetic field dependencies of the activation energy for applied field parallel to *ab* plane and *c* direction.

BaFe_{1.9}Ni_{0.1}As₂ single crystal for *H*||*c*. Flux jumping was observed at 2 K at low magnetic field, similar to what was observed in K doped 122 single crystal.²⁰ The temperature dependence of the superconducting diamagnetic moment of the sample is shown in the inset of Fig. 5. BaFe_{1.9}Ni_{0.1}As₂ single crystal exhibited its superconducting transition temperature at 17.6 K. This value is the same as the *T_c* value from the resistivity measurement. Figure 6 shows the *J_c* calculated by using the Bean model: $J_c = 20\Delta m / (a(1 - a/3b))$ (*a* < *b*), where Δm is the height of the magnetization loop, and *a* and *b* are the length and width of the sample, respectively. *J_c* is as high as 5.4×10^5 and 1.14×10^5 A/cm² at 2 and 10 K in zero magnetic fields, respectively. The estimated *J_c* at 10 K is in good agreement with the *J_c* value of similar compounds.¹³ *J_c* decreases with increasing magnetic field up to 1 T and after that, becomes nearly field independent, which is related to the very high pinning potential in this compound. The second magnetization peak can be seen at *T* = 10 K, possibly due to softening of the

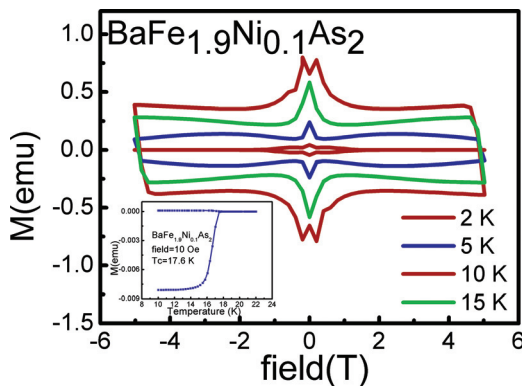


FIG. 5. (Color online) Magnetic field as a function of applied field at *T* = 2, 5, 10, and 15 K. The inset shows the temperature dependence of field cooled and zero fields cooled in a field of 50 Oe for BaFe_{1.9}Ni_{0.1}As₂ single crystal.

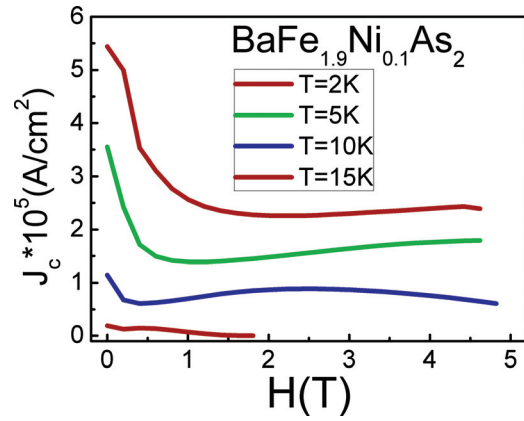


FIG. 6. (Color online) Critical current density vs applied magnetic field at different temperature for BaFe_{1.9}Ni_{0.1}As₂ single crystal.

vortices. At this temperature, vortex can find pinning centers more easily, which results in a higher flow of supercurrent in certain magnetic fields. The applied magnetic field is not high enough to allow the second magnetization peak to be observed at 2 and 5 K. A similar peak effect has been reported for the 122-FeAs family.¹³

In summary, the BaFe_{1.9}Ni_{0.1}As₂ single crystal exhibits high pinning potential, although it has a very small coherence length. It is possible that its nearly isotropic properties are responsible for the high pinning potential value of this compound. A peak effect was observed at *T* = 10 K. Flux jumping occurred at 2 K at very low magnetic field.

This work is supported by the Australian Research Council through ARC Discovery projects DP0558753 and DP1094037.

¹Y. Kamihara *et al.*, *J. Am. Chem. Soc.* **130**, 3296 (2008).

²Q. Huang *et al.*, *Phys. Rev. Lett.* **101**, 257003 (2008).

³Y. Su *et al.*, *Phys. Rev. B* **79**, 064504 (2009).

⁴M. Rotter *et al.*, *Phys. Rev. B* **78**, 020503 (2008).

⁵Y. Qi *et al.*, *New J. Phys.* **10**, 123003 (2008).

⁶H. S. Jeevan *et al.*, *Phys. Rev. B* **78**, 092406 (2008).

⁷K. Sasmal *et al.*, *Phys. Rev. Lett.* **101**, 107007 (2008).

⁸A. S. Sefat *et al.*, *Phys. Rev. Lett.* **101**, 117004 (2008).

⁹P. C. Canfield *et al.*, *Phys. Rev. B* **80**, 060501 (2009).

¹⁰N. Ni *et al.*, *Phys. Rev. B* **80**, 024511 (2009).

¹¹F. Han *et al.*, *Phys. Rev. B* **80**, 024506 (2009).

¹²Z. Bukowski *et al.*, *Phys. Rev. B* **79**, 104521 (2009).

¹³D. L. Sun *et al.*, *Phys. Rev. B* **80**, 144515 (2009).

¹⁴B. Shen *et al.*, *Phys. Rev. B* **81**, 014503.

¹⁵R. Kopeliansky *et al.*, *Phys. Rev. B* **81**, 092504.

¹⁶R. Prozorov *et al.*, *Phys. Rev. B* **78**, 224506 (2008).

¹⁷H. Yang *et al.*, *Appl. Phys. Lett.* **93**, 142506 (2008).

¹⁸A. K. Pramanik *et al.*, *Phys. Rev. B* **82**, 014503 (2010).

¹⁹H. Q. Yuan *et al.*, *Nature* **457**, 565 (2009).

²⁰X. L. Wang *et al.*, *Phys. Rev. B* **82**, 024525 (2010).

²¹L. J. Li *et al.*, *New J. Phys.* **11**, 025008 (2009).

²²E. H. Brandt, *Act. Passive Electron. Compon.* **15**, 193 (1993).

²³Q. Tao *et al.*, *Chin. Phys. Lett.* **26**, 097401 (2009).

²⁴A. Yamamoto *et al.*, *Appl. Phys. Lett.* **94**, 062511 (2009).

²⁵T. T. M. Palstra *et al.*, *Phys. Rev. B* **41**, 6621 (1990).